The structures of neutral transition metal doped silicon clusters, Si_nX (n = 6−9; X = V, Mn)

Pieterjan Claes,[a*] Vu Thi Ngan,[b†] Marko Haertelt,[c] Jonathan T. Lyon,[c,d] André Fielicke,[c] Minh Tho Nguyen,[b] Peter Lievens,[a] and Ewald Janssens[a]

[a] *Laboratory of Solid State Physics and Magnetism, KU Leuven, Celestijnenlaan 200D, B-3001 Leuven, Belgium*

[b] *Department of Chemistry, KU Leuven, Celestijnenlaan 200 F, B-3001 Leuven, Belgium*

[c] *Fritz-Haber-Institut der Max-Planck-Gesellschaft, Faradayweg 4-6, D-14195 Berlin, Germany*

[d] *Department of Natural Sciences, Clayton State University, 2000 Clayton State Boulevard, Morrow, GA 30260, USA*

* *Present address: Departamento de Física Experimental, Instituto de Física, Universidad Nacional Autónoma de México, Mexico-City, Mexico.*

† *Present address: Faculty of Chemistry, Quy Nhon University, Quy Nhon city, Binh Dinh province, Vietnam.*

We present a combined experimental and theoretical investigation of small neutral vanadium and manganese doped silicon clusters Si_nX (n = 6−9, X = V, Mn). These species are studied by infrared multiple photon dissociation and mass spectrometry. Structural identification is achieved by comparison of the experimental data with computed infrared spectra of low-lying isomers using density functional theory at the B3P86/6-311+G(d) level. The assigned structures of the neutral vanadium and manganese doped silicon clusters are compared with their cationic counterparts. In general the neutral and cationic $Si_nV^{0,+}$ and $Si_nMn^{0,+}$ clusters have similar structures, although the position of the capping atoms depend for certain sizes on the charge state. The influence of the charge state on the electronic properties of the clusters is also investigated by analysis of the density of states, the shapes of the molecular orbitals, and NBO charge analysis of the dopant atom.

A) Introduction

The properties of silicon-based clusters attract a great deal of attention because of their importance in both applied and fundamental sciences. In current semiconductor industry, nano-electronic devices are constructed with the use of lithographic techniques. As a result of ongoing miniaturization, this top-down approach reaches fundamental limits and alternative bottom-up approaches using nanometer sized building blocks are considered.[1] Clusters can play a key role in this quest. Thorough knowledge of their size, composition, and charge state dependent properties is essential to create opportunities to construct materials with application-specific features.

The incorporation of a dopant atom is a way to tailor the electronic, magnetic, and optical properties of silicon clusters. Doping with transition metal atoms with unfilled *d*-shells is a promising approach to create clusters with new properties. In particular, one might be able to construct size-specific magnetic silicon clusters.

Recently, charged doped silicon clusters have been studied in great detail via numerous different experimental techniques in combination with theoretical investigations. Structural insight was obtained in photoelectron spectroscopy studies on anionic clusters that monitor the electronic structure[2,3,4,5] and photodissociation experiments that identify sizes or subunits with enhanced stability.[6] Soft X-ray absorption spectroscopy has been used to investigate the local electronic structure of the dopant atom and to measure the HOMO-LUMO gaps of doped silicon clusters.[7,8] More direct structural information about cationic doped silicon clusters has been obtained via infrared spectroscopy.[9,10,11,12]

From an experimental point-of-view, neutral clusters are more difficult to investigate because common mass spectrometric techniques, like mass selection or trapping cannot directly be applied. Experiments on neutral clusters in the gas phase are usually done in a molecular beam and postionization is a prerequisite to detect the clusters. Therefore, the amount of

experimental data on neutral (doped) clusters is limited. On the other hand, several theoretical studies have been conducted on bare[13,14,15,16] and transition metal doped[4,17,18,19] neutral silicon clusters, particularly focusing on the geometry of those species. Few experimental data is available to confirm the predicted structures. Structural determination of neutral Si_n ($n \leq 7$) clusters in cryogenic matrices has been obtained via infrared spectroscopy of clusters produced by co-condensation of silicon atoms with rare gases[20] as well as via Raman spectroscopy[21,22] after mass selection and low-energy deposition. Recently, we identified the geometrical structure of selected small neutral silicon clusters in the gas phase using two different approaches.[23,24] The first one uses a two color ionization scheme, composed of infrared (IR) photo-absorption and ultraviolet (UV) photo-ionization. If the energy of the UV photon is close to the threshold ionization energy of the clusters, prior IR photo-absorption enhances the ionization efficiency after absorption of the UV photon. Scanning the IR photon energy then allows to record the IR absorption spectrum, which was used to identify the geometry of Si_n (n = 6, 7, 9, and 10).[23,24]

The second approach, which is followed in the present work, uses infrared multiple photon dissociation (IR-MPD) of cluster-rare gas complexes in combination with post-ionization. The technique is described in the experimental section and was used before to identify the structures of neutral bare Si_n (n = 8, 9, and 15),[24] cationic bare Si_n^+ (n = 6−21),[9] and cationic metal doped Si clusters.[10,11]

In this paper we discuss the geometry of small neutral vanadium and manganese doped silicon clusters, Si_nV (n = 6−9) and Si_nMn (n = 6, 8, and 9), using infrared multiple photon dissociation of the cluster−Xe complexes combined with DFT calculations at the B3P86/6-311+G(d) level. Vanadium ([Ar] $3d^34s^2$) and manganese ([Ar] $3d^54s^2$) are chosen as dopant atoms because they both have an unfilled 3*d*-shell, but nonetheless show very distinct magnetic properties. We investigate the influence of these dopant atoms on the structure of

the silicon clusters. The identified structures of the neutral doped silicon clusters are compared with their cationic counterparts[10,11] and the influence of the charge state on the geometric and electronic structures of the clusters is analyzed.

B) Experimental and theoretical methods

The far-infrared spectroscopy experiments are performed at the Free Electron Laser for Infrared eXperiments (FELIX) facility of the FOM Institute for Plasma Physics 'Rijnhuizen' in Nieuwegein, the Netherlands.[25] The doped silicon clusters are produced in a two-stage molecular beam setup, containing a dual-target dual-laser vaporization source[26] and a time-of-flight mass spectrometer, which is connected to a beamline of FELIX.[27]

Transition metal doped clusters are formed by ablation of the two target materials using two independent Nd:YAG lasers and subsequent condensation of the ablated atoms in a He atmosphere containing a small fraction (0.6% for Si_nV and 2% for Si_nMn) of isotopically enriched ^{129}Xe. This small portion of xenon atoms in the carrier gas is needed to form the cluster-rare gas complexes, which are used to monitor the light absorption. Isotopically enriched ^{129}Xe is used in order to reduce the number of isotopomers present in the mass spectra. Given the natural isotope distribution of silicon and xenon, mass spectral overlap of the different species present in the molecular beam, $Si_nX_m{\cdot}Xe_p$ (n = 6−17, m = 0−2, p = 0,1, X = V, Mn), would otherwise hamper unique identification from a given mass peak. Thermalization of the clusters and formation of the cluster−rare gas complexes occurs in a cooled extension channel of the source held at a constant temperature of 90 K. The cluster formation stops by expansion into vacuum, which creates a molecular beam. The central part of the molecular beam is skimmed using a 2 mm diameter skimmer. The beam thereafter passes through a second aperture (1 mm diameter), which ensures a good spatial overlap between the molecular beam and the FELIX laser light. The aperture is placed at a potential to deflect charged particles out of the molecular beam. The remaining neutral clusters are then

ionized by a weakly focused beam of vacuum-ultraviolet (VUV) photons of 7.87 eV energy from an F_2 gas laser. For the considered size range of clusters, Si_n (n=6−9), Fuke *et. al.* reported ionization energies in the range of 7.46–7.90 eV.[28] The ionization energy of V and Mn doped clusters is expected not to be significantly higher than that of pure silicon clusters, since the ionization energies of the V atom (6.75 eV) and the Mn atom (7.43 eV) are below that of the Si atom (8.16 eV). The photon fluence of the F_2 gas laser is kept low to avoid photofragmentation and to ensure single photon ionization.[29]

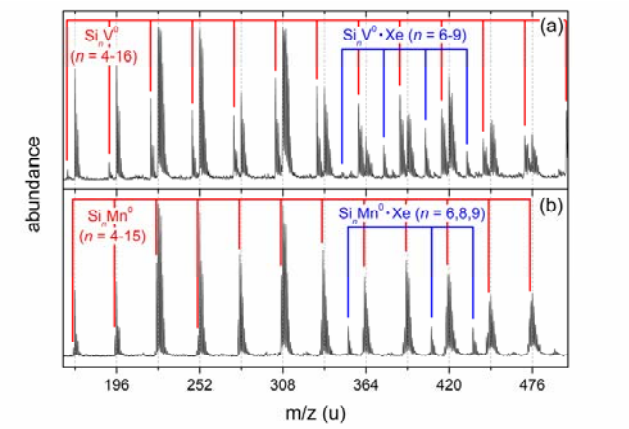

FIG. 1 Typical mass spectra of neutral Si_nV (a) and Si_nMn (b) (n = 4−15) clusters, post-ionized by 7.87 eV photons. The extension channel of the cluster source is held at a constant temperature of 90 K. The gridlines coincide with the bare Si_n clusters. The red and blue lines mark the positions of the Si_nX (X = V, Mn) clusters and their Xe complexes, respectively. The xenon complexes are produced by addition of a small fraction of isotopically enriched ^{129}Xe atoms to the He carrier gas (0.6% and 2% for Si_nV and Si_nMn, respectively).

Typical mass spectra of neutral vanadium and manganese doped silicon clusters are presented in Figure 1. It should be noted that due to different ionization efficiencies, relative intensities of different cluster sizes in the mass spectra (after postionization) may differ from relative intensities in the cluster beam.[28,30] Since relative intensities are not compared with one another, this has no influence on the resulting IR-MPD spectra. Only specific cluster sizes attach a xenon atom and could be postionized under the current experimental conditions, i.e.,

Si_nV (n = 6−9) and Si_nMn (n = 6, 8, 9). For larger sizes Xe attachment might be hampered by the formation of endohedral clusters, where the dopant atom moves inside a silicon cage.[31] For selected sizes the ionization efficiency of the cluster−Xe complex can be low at 7.87 eV. The abundance of postionized Si_7Mn and $Si_7Mn{\cdot}Xe$ is low under the current experimental conditions. The calculated adiabatic ionization energy of Si_7Mn is close to 7.87 eV, while we calculated lower values for Si_6Mn (7.23 eV), Si_8Mn (7.52 eV) and Si_9Mn (7.38 eV). Alternatively the cluster−Xe bond in $Si_7Mn{\cdot}Xe$ may be particularly weak and the complex does not survive on the timescale of the experiment. The mass of Si_nMn differs only 1 u from that of Si_{n+2}. Therefore the IR-MPD spectra of the Si_nMn clusters are recorded on the first isotope of the $Si_nMn{\cdot}Xe$ complexes solely, to exclude mass coincidence with $Si_{n+2}{\cdot}Xe$.

Resonant absorption of IR photons and internal vibrational energy redistribution heat the clusters and may result in evaporation of the weakly bound Xe messenger atom. IR-MPD spectra are obtained in an alternating 'light on − light off' manner, by recording the ion intensities of the cluster−xenon complexes as a function of FELIX photon energy (230−550 cm^{-1}, macropulses of 5−8 μs, linewidth 3−4 cm^{-1}). The intensities of the signal of a specific cluster with and without IR laser light are compared, resulting in depletion spectra from which the final IR absorption spectra can be calculated. These spectra are normalized according to the laser fluence.

To assign the structures of the investigated clusters, the measured IR-MPD spectra of the cluster−xenon complexes are compared with simulated infrared absorption spectra for different low-energetic isomers using density functional theory (DFT). The calculations are performed using the B3P86 hybrid functional and the 6-311+G(d) basis set. The B3P86 functional is composed of Becke's hybrid 3-parameter exchange and the P86 non-local correlation,[32,33] and has the same percentage of the exact Hartree-Fock exchange (20%) as B3LYP. The B3P86 functional was selected, because it was shown to predict the infrared

spectra of cationic Si_nMn^+ (n = 6−16) clusters best, without the need for a scaling factor.[11] The initial geometries for the structural optimization are selected on the basis of the known isomers of cationic Si_nV^+ and Si_nMn^+ [10,11] and structures derived from bare Si_n clusters[23,24] where the dopant atom is added to the surface or substitutes an atom of the silicon framework. All the calculations are performed using the Gaussian 03 package.[34] Atomic charges and local magnetic moments are evaluated based on natural population analysis which is performed at the same level of theory using the NBO 5.G program.[35] Simulated infrared absorption spectra are folded with a Gaussian lineshape of 3 cm^{-1} full width at half maximum (FWHM) corresponding to the linewidth of the infrared light source.

C) Results and Discussion

The following discussion is organized in three parts. First, the IR-MPD spectra of neutral Si_nV and Si_nMn are presented and compared with the infrared absorption spectra of the computed lowest energy isomers. Secondly, the structures and growth mechanisms of the neutral clusters are compared with their cationic counterparts. Finally, the influence of the added electron (from cation to neutral) on the electronic structure of $Si_nV^{+,0}$ and $Si_nMn^{+,0}$ is discussed.

To assign the structures of the clusters using the IR-MPD spectra of the cluster−xenon complexes, the influence of the xenon messenger atom is explicitly taken into account in the computed harmonic vibrational spectra of the predicted lowest-energy isomers. The computed harmonic vibrational spectra of the lowest-energy isomer without Xe messenger atom are shown in the supplementary material.[36] Comparing the harmonic absorption spectrum of the lowest-energy isomer with and without xenon attached shows that the xenon might induce small shifts in the energy of some vibrational modes (typically less than 15 cm^{-1}). On the other hand, the xenon attachment can have a significant effect on the intensity of the infrared absorption bands. The calculations show for all investigated clusters that the Xe messenger

atom binds to the transition metal dopant atom. The strengths of Xe−V and Xe−Mn bonds calculated by comparison of the total energies of the Si_nX clusters and the Si_nX·Xe complexes are in the range of 0.2−0.3 eV. Earlier studies have shown that Xe binding energies on pure Si_n clusters are weaker (of the order of 0.1 eV),[9,24] with the exception of Si_4^+ for which a Xe binding energy of 0.30 eV was found.[37] The addition of Xe has a marginal effect on the relative ordering of the isomers (taking into account a typical uncertainty of the computational method). It should, however, be noted that the used B3P86 level of theory does not explicitly describes long range van der Waals interactions.

Before making a detailed comparison of the IR-MPD spectra with the infrared absorption spectra we remark that a perfect agreement between theory and experiment cannot be expected for several reasons. The calculations use a harmonic single photon approach, whereas the IR-MPD experiment is a multiphoton experiment and potentials are anharmonic. Anharmonicities and multiphoton effects result in shifts between the absorption and the fragmentation spectra and can have a significant effect on the intensities of the bands.[38] Moreover, DFT approaches have difficulties to properly describe influence of the cluster−Xe bond on the infrared spectrum. A good match between theory and experiment usually implies that the number of infrared active bands is correctly reproduced (although near degeneracy might make it difficult to count), and that vibrational frequencies are predicted with an accuracy better than about 5%. Relative intensities of bands can be, however, difficult to reproduce using a harmonic single photon approximation.

C.1) Infrared absorption spectra of Si_nV (n = 6−9)

A comparison of the IR-MPD spectra of the Si_nV·Xe complexes (n = 6−9) and the corresponding computed harmonic vibrational spectra of the predicted lowest-energy isomers at the B3P86/6-311+G(d) level of theory is presented in Figure 2. The geometric structures of

other low-energetic isomers and their corresponding infrared spectra are shown in the supplementary material.[36]

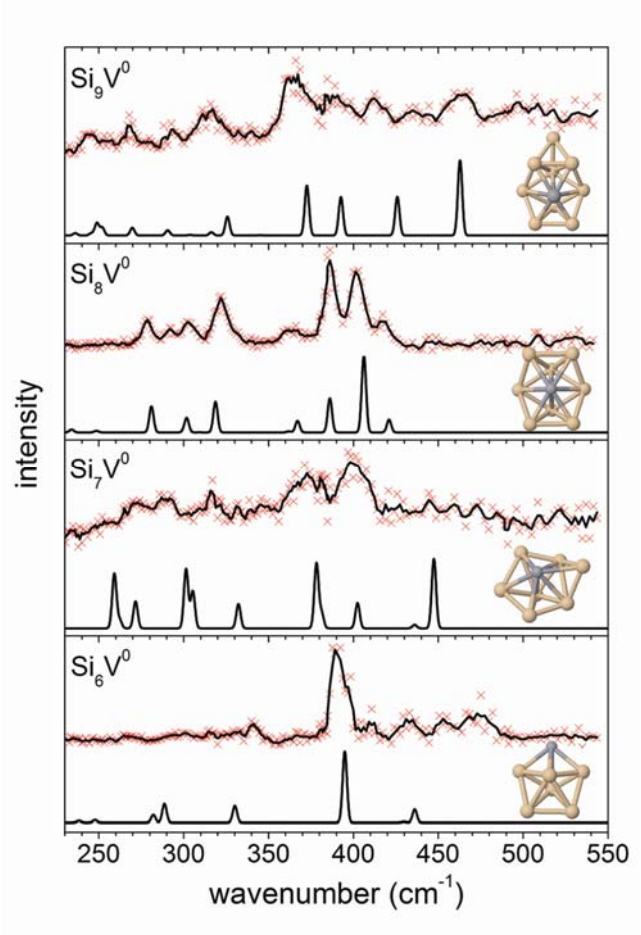

FIG. 2 IR-MPD spectra (upper traces) of $Si_nV{\cdot}Xe$ complexes (n = 6−9) and the corresponding calculated vibrational spectra of the xenon complexes of the lowest-energy isomers (lower traces). The assigned geometries are presented as insets. The experimental data points (red crosses) are overlaid with a three-point running average. The computed infrared spectra are calculated at the B3P86/6-311+G(d) level.

Notably, the overall shapes of the experimental spectra for the different sizes are quite different. In particular the observed bandwidths can be rather different, e.g., compare Si_7V and Si_8V. Since the depletion spectra of all cluster sizes for a given dopant atom are measured simultaneously, the different bandwidths cannot be related to changes in the spectral bandwidth of the IR source. One possibility for the broader bands might be the presence of isomers with overlapping bands that could lead to a blurring of the experimental spectrum.

We have, however, no clear indication for this from the theoretical studies. Another reason might be a fluxional behavior as previously observed for certain systems, e.g. for $Si_{16}V^+$.[12]

Si_6V The IR-MPD spectrum of neutral Si_6V, measured on the $Si_6V{\cdot}Xe$ complex, is characterized by one intense absorption band centered at 390 cm^{-1}. Less intense features at lower and higher wavenumbers are also visible. The calculated ground state is a quartet and its xenon complex fits the experimental infrared absorption spectrum. The lowest-energy isomer is a C_{2v} pentagonal bipyramid structure with an equatorial vanadium atom and the IR spectrum of the xenon complex shows an intense band at 394 cm^{-1}. Smaller contributions at 289, 330, and 436 cm^{-1} could represent the weak peaks in the experimental spectrum.

Si_7V The calculated IR spectrum of the lowest-energy isomer of $Si_7V{\cdot}Xe$ and the corresponding IR-MPD spectrum are shown in Figure 2. Several broad absorption features are measured between 250 and 410 cm^{-1}. The calculated absorption spectrum of the xenon complex of the lowest-energy structure, a face-capped pentagonal bipyramid with C_s symmetry in a doublet state, shows infrared active bands within the range of the experimentally observed bands, except for the band at the highest frequency (447 cm^{-1}). The lowest frequency bands do not show a conclusive match and the overall intensity pattern fits less well. However, also higher energy isomers do not give a better match (see supplementary material [36]). The cationic counterpart, Si_7V^+, was also found to be a face-capped pentagonal bipyramid, although the position of the capping silicon atom differs. In the cationic Si_7V^+ this atom caps an 'all silicon' face,[10] while the capping atom for the neutral Si_7V is located on a V−Si−Si face.

Si_8V This size shows, different to $Si_7V{\cdot}Xe$, a distinct experimental spectrum with good signal-to-noise ratio and relatively sharp bands with a FWHM of around 10 cm^{-1}. A very good agreement between the experiment and the computations is found for a double face-capped pentagonal bipyramidal structure (C_{2v}) in a doublet state, which is also calculated to be the

lowest-energy isomer. Here, the vanadium atom occupies an eightfold coordinated position and the cluster has only triangular faces. The calculated band positions and their relative intensities correspond nicely with the experimental spectrum. The minor deviation around 300 cm^{-1}, where the experimental spectrum has two low intensity bands and the calculated spectrum only one, most likely is related to an underestimation of the frequency differences between the close lying peaks at 295, 298, and 302 cm^{-1} in the calculated spectrum. Higher-energy isomers, built up by capping the pentagonal bipyramid structure of Si_8V, do not show good correspondence with the experiment (see supplementary material [36]), assuring that the double face-capped pentagonal bipyramidal structure is indeed the isomer that is present in the molecular beam.

Si_9V The experimental IR-MPD spectrum of $Si_9V{\cdot}Xe$ show broader and less pronounced bands than that of $Si_8V{\cdot}Xe$. The lowest-energy structure found, electronically a doublet, fits the experiment best in many details. This structure is obtained by capping one of the 'all silicon' faces of Si_8V, and is similar to the tricapped pentagonal bipyramid structure of Si_9V^+,[10] however with a small distortion along the pentagonal ring. The vanadium atom remains 8-fold coordinated while the extra silicon atom gives the onset for cage formation at larger sizes, towards an icosahedral structure with the dopant atom inside the cage. The experimental spectrum is well reproduced by this isomer, though the presence of multiple isomers cannot be excluded. Between 410 and 450 cm^{-1} experimentally two peaks are seen but only a single peak is predicted for the lowest-energy isomer. Two slightly higher lying isomers iso 2 [+0.09 eV] and iso 3 [+0.11 eV] have bands in these ranges (see supplementary material [36]) and their additional presence (one or both) could explain the remaining experimental bands.

Summarizing, we find a good agreement between theory and experiment for Si_6V and Si_8V. The agreement for Si_9V is reasonable, though the presence of additional isomers cannot be excluded. The structural assignment of Si_7V is not conclusive.

C.2) Infrared absorption spectra of Si_nMn (n = 6, 8 and 9)

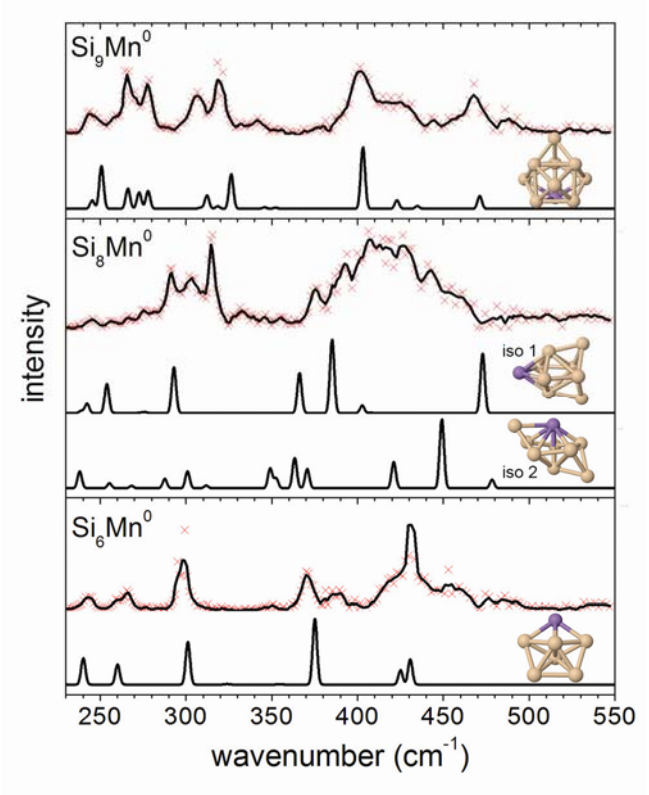

FIG. 3 IR-MPD spectra (upper traces) of $Si_nMn{\cdot}Xe$ complexes (n = 6, 8, 9) and the corresponding calculated vibrational spectra of the xenon complexes of the lowest-energy isomers (lower traces). For Si_8Mn, the second lowest-lying isomer is also presented. The geometries are shown as insets next to their corresponding computed vibrational spectra. The experimental data points (red crosses) are overlaid with a three-point running average. The computed infrared spectra are calculated at the B3P86/6-311+G(d) level.

The IR-MPD spectra of the $Si_nMn{\cdot}Xe$ complexes (n = 6, 8, and 9) are compared with the computed harmonic vibrational spectra of the lowest-energy isomers in Figure 3. For Si_8Mn, no definite structural assignment could be made based on a single isomer (see below), therefore the second lowest-energy isomer, which is only 0.16 eV higher in energy, is

presented in addition. No experimental IR-MPD spectrum for $Si_7Mn{\cdot}Xe$ could be recorded, as it is not abundant in the mass spectrum, probably because the ionization energy of $Si_7Mn{\cdot}Xe$ is higher than 7.87 eV (see above).

Si_6Mn A good agreement is found between the IR-MPD spectrum of $Si_6Mn{\cdot}Xe$ and the calculated spectrum of the lowest-energy isomer, a sextet state with a C_{2v} pentagonal bipyramid structure where the Mn atom takes one of the equatorial positions of the pentagon. The low energy part of the experimental spectrum (below 380 cm^{-1}) is well reproduced by the calculations. The higher energy part of the spectrum is dominated by a strong narrow band at 431 cm^{-1} and can be related to a calculated double peak of similar frequency. Additional features in the IR-MPD spectrum at 388 cm^{-1} and around 455 cm^{-1} are not explained by this structure and point to the possible presence of an additional (still unidentified) isomer.

Si_8Mn The IR-MPD spectrum of $Si_8Mn{\cdot}Xe$ has two main absorption regions: the low-energy region consisting of three clear peaks at 292, 303, and 314 cm^{-1}, and a high-energy region between 375 and 465 cm^{-1}. Many structural isomers are located (see supplementary material [36]), but none shows a one-to-one agreement with the experiment. A combination of the two calculated lowest-lying isomers (iso 1−sextet [C_s, 0 eV] and iso 2−quartet [C_1, +0.16 eV], both bicapped pentagonal bipyramids) might explain the absorption spectrum in the low-energy region, although the infrared active modes of iso 2 have much lower intensities. The high-energy region cannot be explained by a coexistence of these two isomers. Therefore, no conclusive assignment can be made for Si_8Mn, which might imply that the correct isomer has not been found yet. In the following discussion, both lowest-lying isomers will be considered.

Si_9Mn The IR-MPD spectrum of $Si_9Mn{\cdot}Xe$ is characterized by several distinct bands that are well reproduced by the infrared spectrum of the computed lowest-energy isomer. The assigned isomer is a sextet having a symmetry broken tetracapped trigonal prism structure,

similar to the structure found for the bare Si_{10}^+ with the Mn atom substituting a Si atom of the trigonal prism.[9]

Summarizing, the structural assignment of Si_6Mn and Si_9Mn is conclusive, though for Si_6Mn the presence of a second isomer cannot be excluded. For Si_8Mn we cannot be sure that the correct isomer has been identified.

C.3 Influence of the charge state on the electronic structure of $Si_nV^{+,0}$ and $Si_nMn^{+,0}$

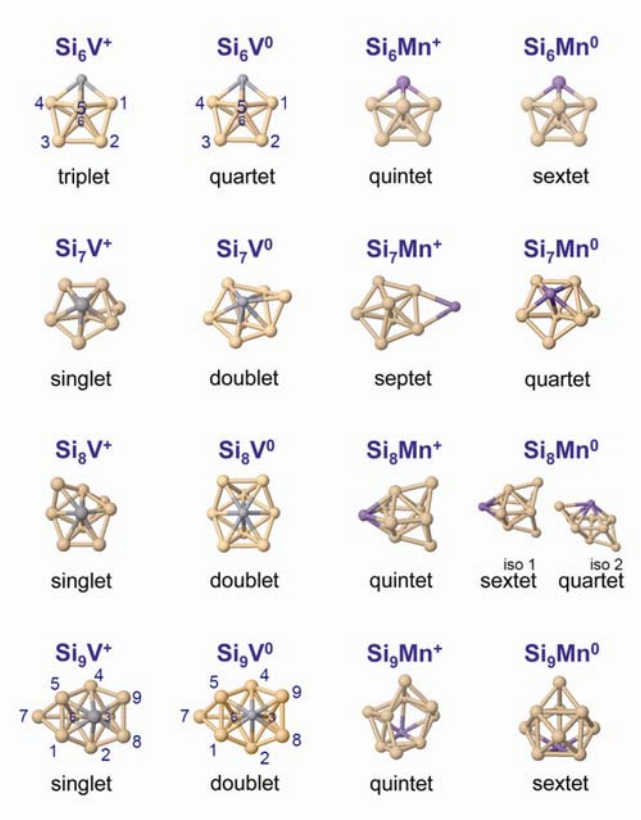

FIG. 4 Overview of the assigned structures of neutral and cationic clusters $Si_nX^{+,0}$ (n = 6−9; X = V, Mn). The structure presented for Si_7Mn^0 corresponds to the calculated lowest-energy isomer. The structures of the cationic Si_nV^+ and Si_nMn^+ are taken from ref. [10] and ref. [11], respectively. The Si atoms numbering is used in the discussion on the influence of the charge state.

A population analysis is performed on the basis of the density of states (DOS) of both charge states. Atomic charges, local magnetic moments on the dopant atom, and the energy gaps between the highest occupied molecular orbital (HOMO) and the lowest unoccupied molecular orbital (LUMO) are calculated. The HOMO-LUMO gap, in the case of open

electronic shell systems, is computed between the highest of the HOMOs and the lowest of the LUMOs, regardless of the spin type. For all studied clusters, except Si_7Mn (related to the particular magnetic structure of Si_7Mn^+),[11] the electron added when going from the cation to the neutral occupies an orbital corresponding to the majority (alpha) spins. This follows from the singlet-doublet, triplet-quartet, and quintet-sextet transitions upon electron addition. Therefore, in the following, the DOS is discussed by considering the majority spin orbitals solely.

For $Si_6V^{+,0}$ (and also for $Si_9V^{+,0}$) the HOMO and LUMO levels are majority spin orbitals and the neutral and cationic clusters have a similar structure. As a result their electronic structure is very similar with exception of the occupation of the frontier orbitals. It is found that the LUMO of the cation is similar to the HOMO of the neutral cluster, as is visualized by the molecular majority spin orbitals in Figure 5. Such a behavior can only happen when the structures of both the cation and neutral are similar and when the HOMO and LUMO of the cation have the same spin. The LUMO of Si_6V^+ consists of 63% V-*d*, 17.5% Si-5,6-*p*, 5% Si-5,6-*s*, 9.6% Si-2,3-*p* , which is very alike to the HOMO of Si_6V^0 (62% V-*d*, 18.5% Si-5,6-*p*, 7.2% Si-5,6-*s*, 8.2% Si-2,3-*p*). The atom numbering is represented in Figure 4. Similarly, the LUMO of and Si_9V^+ (8.3% V-*d*, 30% Si-1,5-*s*, 26.4% Si-2,4-*s*, 11.4% Si-8,9-*s*, 8% Si-1,5-*p*, 6.8% Si-2,4-*p)* resembles the highest SOMO of Si_9V^0 (8.8% V-*d*, 30.4% Si-1,5-*s*, 23.6% Si-2,4-*s*, 12% Si-8,9-*s*, 8.2% Si-1,5-*p*, 7.4% Si-2,4-*p*).

NBO local charge analysis demonstrate that for most studied sizes the charge on transition metal dopant atom does not change significantly upon electron addition (see Table I). Si_8V is an exception in this respect as the vanadium atom receives a large fraction of the added electron, in comparison with the other clusters.

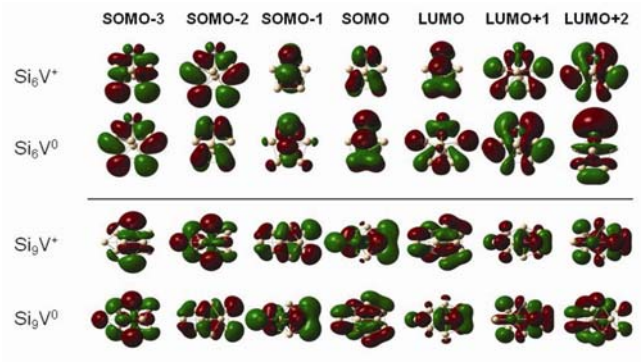

FIG. 5 An overview of the frontier molecular á-orbitals of $Si_6V^{+,0}$ and $Si_9V^{+,0}$. The geometry of the clusters is shown in Figure 4.

Table I. Local atomic charges (in *e*) and local spin magnetic moment (in μ_B) on the dopant atom for the $Si_nX^{+,0}$ (n = 6−9; X = V, Mn) structures shown in Figure 4 using natural population analysis. HOMO-LUMO gaps (in eV) calculated at the B3P86/6-311+G(d) level of theory are also given.

	Atomic charge on dopant atom (*e*)		Local magnetic moment on dopant atom (μ_B)		HOMO-LUMO gap (eV)	
size	cation	neutral	cation	neutral		
$Si_6V^{+,0}$	+0.46	+0.51	+2.5	+3.3	0.699	2.100
$Si_7V^{+,0}$	-0.17	-0.22	0.0	+1.4	1.053	1.673
$Si_8V^{+,0}$	-0.41	-0.78	0.0	-0.4	1.138	1.532
$Si_9V^{+,0}$	-0.77	-0.62	0.0	+1.4	0.881	1.733
$Si_6Mn^{+,0}$	+0.96	+0.91	+4.3	+4.4	2.034	1.701
$Si_7Mn^{+,0}$	+0.83	+0.42	+5.7	+3.9	1.885	1.683
$Si_8Mn^{+,0}$	+0.93	+0.84 (iso 1)	+4.2	+4.2	1.705	1.759 (iso 1)
		+0.33 (iso 2)		+3.8		+1.683 (iso 2)
$Si_9Mn^{+,0}$	+0.80	+0.82	+4.2	+4.3	1.823	2.017

It was recently demonstrated that the manganese dopant atoms in cationic Si_nMn^+ (n = 6−10) clusters carry large local magnetic moments of 4 μ_B to 6 μ_B.[11] It was also found that the structures of Si_nMn^+ (n = 6−10) can markedly be described as substitution derivatives of the bare Si_{n+1}^+ cations in spite of the very different electronic nature of Si and Mn.[9,11] The comparison of neutral and cationic $Si_nMn^{+,0}$ in Figure 4 and the results of the natural population analysis in Table I demonstrates that, with the exception of Si_7Mn, also the neutral

Si_nMn clusters are substitution derivatives of Si_n^+ with a large local magnetic moment on the manganese dopant atom.

D Conclusion

The structures of Si_nV (n = 6−9) and Si_nMn (n = 6, 8, 9) are identified by comparing measured IR-MPD spectra of the cluster-Xe complexes with simulated infrared absorption spectra for different structural isomers found at the B3P86/6-311+G(d) level of theory. For all clusters, the best agreement was obtained with the located lowest energy isomers. Although no definite assignment could be made for Si_8Mn. The structures of the neutral clusters are compared with their cationic counterparts from earlier studies.[10,11] The geometric structures of the neutral exohedrally doped silicon clusters do not differ much from their cationic counterparts, but, slight differences in positions of capping atoms are found. This similarity is also reflected in the electronic structure where the added electron will occupy the majority spins LUMO orbital of the cationic species. The analysis of the NBO charge on the transition metal atom shows that most of the extra electron, when changing charge state, is distributed over the entire silicon framework.

Acknowledgements

We gratefully acknowledge the support of the Stichting voor Fundamenteel Onderzoek der Materie (FOM) for providing beam time on FELIX. The authors thank the FELIX staff for their skillful assistance, in particular Dr. B. Redlich and Dr. A. F. G. van der Meer. P. C. thanks D. Aguilar for technical support. This work is supported by the Fund for Scientific Research-Flanders (FWO), by the Flemish Concerted Action (Contract No. GOA/2009/06), and by the Deutsche Forschungsgemeinschaft within FOR 1282 (FI 893/4-1). P. C. thanks the Institute for the Promotion of Innovation by Science and Technology in Flanders (IWT) for financial support, V. T. N thanks the KU Leuven for a postdoctoral fellowship, and J. T. L. thanks financial support from the Alexander von Humboldt Foundation.

References

[1] D. Vuillaume, Proc. of the IEEE **98**, 2111 (2010).

[2] A. Grubisic, Y. J. Ko, H. Wang, and K. H. Bowen, J. Am. Chem. Soc. **131**, 10783 (2009).

[3] K. Koyasu, J. Atobe, M. Akutsu, M. Mitsui, and A. Nakajima, J. Phys. Chem. A **111**, 42 (2007).

[4] H.-G. Xu, Z.-G. Zhang, Y. Feng, J. Yuan, Y. Zhao, and W. Zheng, Chem. Phys. Lett. **487**, 204 (2010).

[5] H.-G. Xu, M. M. Wu, Z.-G. Zhang, J. Yuan, Q. Sun, and W. Zheng, J. Chem. Phys. **136**, 104308 (2012).

[6] J. B. Jaeger, T. D. Jaeger, and M. A. Duncan, J. Phys. Chem. A **110**, 9310 (2006).

[7] J.T. Lau, K. Hirsch, Ph. Klar, A. Langenberg, F. Lofink, R. Richter, J. Rittman, M. Vogel, V. Zamudio-Bayer, T. Möller, and B. von Issendorff, Phys. Rev. A **79**, 053201 (2009).

[8] J. T. Lau, M. Vogel, A. Langenberg, K. Hirsch, J. Rittmann, V. Zamudio-Bayer, T. Möller, and B. von Issendorff, J. Chem. Phys. **34**, 041102 (2011).

[9] J. T. Lyon, P. Gruene, A. Fielicke, G. Meijer, E. Janssens, P. Claes, and P. Lievens, J. Am. Chem. Soc. **131**, 1115 (2009).

[10] V. T. Ngan, P. Gruene, P. Claes, E. Janssens, A. Fielicke, M. T. Nguyen, and P. Lievens, J. Am. Chem. Soc. **132**, 15589 (2010).

[11] V. T. Ngan, E. Janssens, P. Claes, J. T. Lyon, A. Fielicke, M. T. Nguyen, and P. Lievens, Chem. Eur. J. **18**, 15788 (2012).

[12] P. Claes, E. Janssens, V. T. Ngan, P. Gruene, J. T. Lyon, D. J. Harding, A. Fielicke, M. T. Nguyen, and P. Lievens, Phys. Rev. Lett. **107**, 173401 (2011).

[13] S. Goedecker, W. Hellman, and T. Lenosky, Phys. Rev. Lett. **95**, 055501 (2005).

[14] W. Qin, W.-C. Lu, L.-Z. Zhao, Q.-J. Zang, C. Z. Wang, and K. M. Ho, J. Phys.: Condens. Matter **21**, 455501 (2009).

[15] F. Avaltroni and C. Corminboeuf, J. Comput. Chem. **32**, 1869 (2011).

[16] H. U. Rehman, M. Springborg, and Y. Dong, J. Phys. Chem. A **115**, 2005 (2011).

[17] Y.-Z. Lan and Y.-L. Feng, Phys. Rev. A **79**, 033201 (2009).

[18] J. U. Reveles and S. N. Khanna, Phys. Rev. B **72**, 165413 (2005).

[19] J. Li, G. H. Wang, C. H. Yao, Y. W. Mu, J. G. Wan, and M. Han, J. Chem. Phys. **130**, 164514 (2009).

[20] S. Li, R.J. Van Zee, J.W. Weltner, and K. Raghavachari, Chem. Phys. Lett. **243**, 275 (1995).

[21] E. C. Honea, A. Ogura, D. R. Peale, C. Felix, C. A. Murray, K. Raghavachari, W. O. Sprenger, M. F. Harrold, and W. L. Brown, J. Chem. Phys. **110**, 12161 (1999).

[22] E. C. Honea, A. Ogura, C. A. Murray, K. Raghavachari, W. O. Sprenger, M. F. Harrold, and W. L. Brown, Nature (London) **366**, 42 (1993).

[23] A. Fielicke, J. T. Lyon, M. Haertelt, G. Meijer, P. Claes, J. de Haeck, and P. Lievens, J. Chem. Phys. **131**, 171105 (2009).

[24] M. Haertelt, J. T. Lyon, P. Claes, J. de Haeck, P. Lievens, and A. Fielicke, J. Chem. Phys. **136**, 064301 (2012).

[25] D. Oepts, A. F. G. van der Meer, and P. W. van Amersfoort, Infrared Phys. Technol. **36**, 297 (1995).

[26] W. Bouwen, P. Thoen, F. Vanhoutte, S. Bouckaert, F. Despa, H. Weidele, R. E. Silverans, and P. Lievens, Rev. Sci. Instrum. **71**, 54 (2000).

[27] A. Fielicke, G. von Helden, and G. Meijer, Eur. Phys. J. D **34**, 83 (1999).

[28] K. Fuke, K. Tsukamoto, F. Misaizu, and M. Sanekata, J. Chem. Phys. **99**, 7807 (1993).

[29] D. J. Trevor, D. M. Cox, K. C. Reichmann, R. O. Brickman, and A. Kaldor, J. Phys. Chem. **91**, 2598 (1987).

[30] J. De Haeck, T. B. Tai, S. Bhattacharyya, H. T. Le, E. Janssens, M. T. Nguyen, and P. Lievens, Phys.Chem. Chem. Phys. 15, 5151 (2013).

[31] E. Janssens, P. Gruene, G. Meijer, L. Wöste, P. Lievens, and A. Fielicke, Phys. Rev. Lett. **99**, 063401 (2007).

[32] J. P. Perdew, Phys. Rev. B **33**, 8822 (1986).

[33] A. D. Becke, J. Chem. Phys. **98**, 5648 (1993).

[34] Gaussian 03, Revision C.02, M. J. Frisch, *et al*., Gaussian, Inc., Wallingford CT (2004).

[35] E. D. Glendening, *et al*., NBO 5.G. (Theoretical Chemistry Institute, University of Wisconsin, Madison, WI) (2004).

[36] See supplementary material at [URL to be inserted] for a more detailed comparison between the infrared absorption spectra of several low-energetic Si_nX ($n = 6-9$; X = V, Mn) isomers, calculated at the B3P86/6-311+G(d) level of theory, and the experimental IR-MPD spectra recorded on the corresponding Si_nX·Xe complexes. Also low-lying isomers of Si_7Mn calculated at the same level of theory are presented.

[37] M. Savoca, J. Langer, D. J. Harding, O. Dopfer, and A. Fielicke, Chem. Phys. Lett. **557**, 49 (2013).

[38] F. Calvo and P. Parneix, ChemPhysChem **13**, 212 (2012).